DOE-GTRC-05596

FINAL TECHNICAL REPORT

11/24/2014

1. Title:

Collaborative Research: Process-Resolving Decomposition of the Global Temperature Response to Modes of Low Frequency Variability in a Changing Climate

2. Reporting Period:

09/15/2010 – 09/14/2014

3. Funding Period:

09/15/2010 – 09/14/2014
Contract number: DE-SC0005596

4. PI/Co-PI Information:

Dr. Yi Deng (PI)
School of Earth and Atmospheric Sciences
Georgia Institute of Technology
311 Ferst Drive, Atlanta, GA 30332-0340
404-385-1821, yi.deng@eas.gatech.edu

5. Project Synopsis:

El Niño-Southern Oscillation (ENSO) and Annular Modes (AMs) represent respectively the most important modes of low frequency variability in the tropical and extratropical circulations. The projection of future changes in the ENSO and AM variability, however, remains highly uncertain with the state-of-the-science coupled general circulation models. The proposed research aims to identify sources of such uncertainty and establish a set of process-resolving, quantitative evaluations of the ENSO and AM variability in the model-simulated present climate and in the existing predictions of the future climate. The proposed process-resolving evaluations are based on a feedback analysis method originally formulated by one of the PIs (Collaborative PI Dr. Ming Cai at the Florida State University), which is capable of partitioning 3D temperature anomalies/perturbations into components linked to 1) radiation-related thermodynamic processes such as cloud and water vapor feedbacks, 2) local dynamical processes including convection and turbulent/diffusive energy transfer and 3) non-local dynamical processes such as the horizontal energy transport in the oceans and atmosphere. Taking advantage of the high-resolution reanalysis products (such as the ERA Interim) and multi-model ensemble products from the Coupled Model Intercomparison Project Phase 5 (CMIP5), we will conduct a process-resolving decomposition of the global 3D temperature (including SST) response to the ENSO and AM variability in the observation (reanalysis) and in the preindustrial, historical and future climate simulated by the CMIP5 models. Specific research tasks include 1) identifying the model-observation discrepancies in the global temperature response to ENSO and AM variability and attributing such discrepancies to specific feedback processes, 2) delineating the influence of anthropogenic radiative forcing on the key feedback processes operating on ENSO and AM variability and quantifying their relative contributions to the changes in the temperature anomalies associated with different phases of ENSO and AMs, and 3) investigating the linkages between model feedback processes that lead to inter-model differences in time-mean temperature projection and model feedback processes that cause inter-model differences in the simulated ENSO and AM temperature response.

6. Primary Research and Development Activities

Summary of Research Activities

Research activities performed at Georgia Tech include: 1) download of the ERA-Interim and CMIP5 model data into the local cluster, 2) construction of composite atmospheric and surface state representative of ENSO+, ENSO-, NAM+, and NAM- phases for CFRAM analysis, 3) performing CFRAM calculations for ENSO and NAM variability using ERA-interim data and CMIP5 model output, and 4) write scientific papers to summarize key results and present new findings to the broader climate research community.

At Georgia Tech, we have published **15** peer-reviewed journal articles (including one to be submitted soon) that acknowledge the support from this DOE grant (See Section 8 for details). The grant also supported travels for **9** conference/workshop presentations.

Summary of Key Research Findings

1. **Process-level attribution of 3D atmospheric and surface temperature anomalies related to ENSO variability in reanalysis and in CMIP5 models**

   Deng et al. (2012) reported an attribution analysis that quantifies addible contributions to the observed temperature anomalies from radiative and non-radiative processes in terms of both amplitude and spatial-pattern for the two most prominent surface temperature patterns in an El Niño winter. One is the El Niño SST pattern consisting of warming SST anomalies over the eastern equatorial Pacific basin surrounded by cooling SST anomalies in the western and subtropical Pacific, and the other is a tri-pole surface temperature anomaly characteristic of a positive Pacific-North American (PNA) teleconnection pattern (Figure 1). The total surface temperature anomalies in a composite El Niño winter are first decomposed with CFRAM into partial temperature changes due to various feedbacks (Figure 2). The subsequent attribution analysis is based upon the definition of a pattern-amplitude-projection (PAP) coefficient and summarized in Figure 3. Out of the mean amplitude of 0.78 K of the El Niño SST pattern, oceanic dynamics and heat storage term alone contributes to 2.34 K. Water vapor feedback adds another 1.6 K whereas both cloud and atmospheric dynamical feedbacks are negative, reducing the mean amplitude by 2.02 K and 1.07 K, respectively. Atmospheric dynamical feedback contributes more than 50% (0.73 K) of the mean amplitude (1.32 K) of the PNA surface temperature pattern. Water vapor and surface albedo feedbacks contribute 0.34 K and 0.13 K, respectively. The surface processes, including oceanic dynamics in the North Pacific, heat storage anomalies and surface sensible/latent heat flux anomalies of ocean and land, also contribute positively to the PNA surface temperature pattern (about 0.14 K). Cloud and ozone feedback, although very weak, act to oppose the PNA surface temperature anomaly.

   Reporting the attribution results for ENSO-related 3D atmospheric temperature responses, Park et al. (2012) confirms that atmospheric dynamics plays distinctly different roles in establishing the tropical and extratropical temperature response to El Niño. For example, Figure 4 shows the partitioning of surface and atmospheric temperature anomalies at different vertical levels into contributions from various feedback processes for 3 latitudinal zones: tropics, midlatitudes and polar region. The outstanding features include the opposite effect of cloud feedback between mid-lower troposphere and upper-troposphere-lower-stratosphere in the tropics, and opposite effect of atmospheric dynamical feedback between troposphere and stratosphere in midlatitudes. In summary, the atmospheric dynamics serves as a primary negative feedback to the tropical (tropospheric) warming by transporting out of the tropics excessive energy production associated with oceanic dynamical forcing. In the northern extratropics, it is the main forcing of atmospheric temperature changes and also modulates surface temperatures via longwave radiative heating and cooling. This provides an alternative view of the “atmospheric bridge” mechanism from the perspective of local energetics and temperature feedback attribution. Substantial tropospheric cooling over the eastern North Pacific is found to be collectively contributed by water vapor, cloud, and atmospheric dynamical feedbacks, driven at least partly by the equatorward shift of the Pacific storm track during El Niño. Polar stratospheric warming (cooling), largely due to atmospheric dynamics, is seen over the Eurasian-Pacific (Atlantic) sector, with ozone feedback contributing significantly to the mid-stratospheric cooling over the Atlantic sector. Water vapor (atmospheric dynamical) feedback has an overall warming (cooling) effect throughout the tropical troposphere, and cloud feedback cools (warms) the tropical lower to middle (upper) troposphere. Atmospheric dynamics induces stratospheric warming over the entire northern extratropics and drives over northern midlatitudes (high latitudes) a tropospheric cooling (warming) that generally intensifies with altitude.

When applied to ENSO variability in a series of CMIP5 models’ historical climate simulations, CFRAM reveals that even though majority of models simulate realistic temperature anomalies associated with ENSO variability, the relative contributions to these temperature anomalies from various radiative and dynamical processes are drastically different across different models and between model and observation. For example, Figure 5 shows the partial temperature changes due to specific feedback processes relative to the total temperature change over the equatorial Pacific during El Niño in observations and in multiple CMIP5 models. Despite the multi-model ensemble average converging to the observation, significant biases exist in individual model representations. Figure 6 is the same as Figure 5 except for the PNA region. It is clear that in the extratropics even the multi-model average does not show any sign of convergence for the forcing of local temperature anomalies at the process-level. We are currently preparing a manuscript to report these findings and discuss their implications for efforts of future model development (Park et al. 2014b).

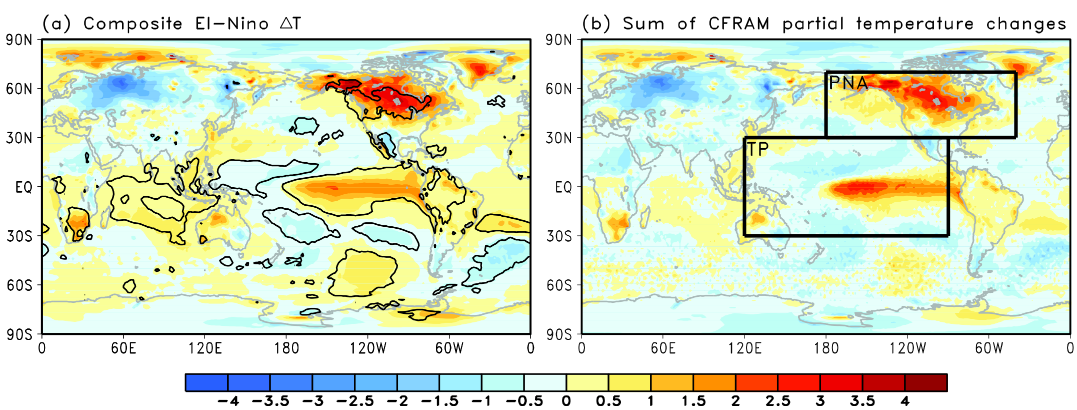

Fig. 1. (a) The global surface temperature anomalies in a canonical El Niño winter (DJF), expressed in terms of the difference between the composite El Niño state and the composite ENSO-neutral state; (b) the sum of partial temperature anomalies derived through CFRAM. Unit is *K*. Contour in (a) indicates 90% level of statistical significance. (Adapted from Deng et al. 2012)

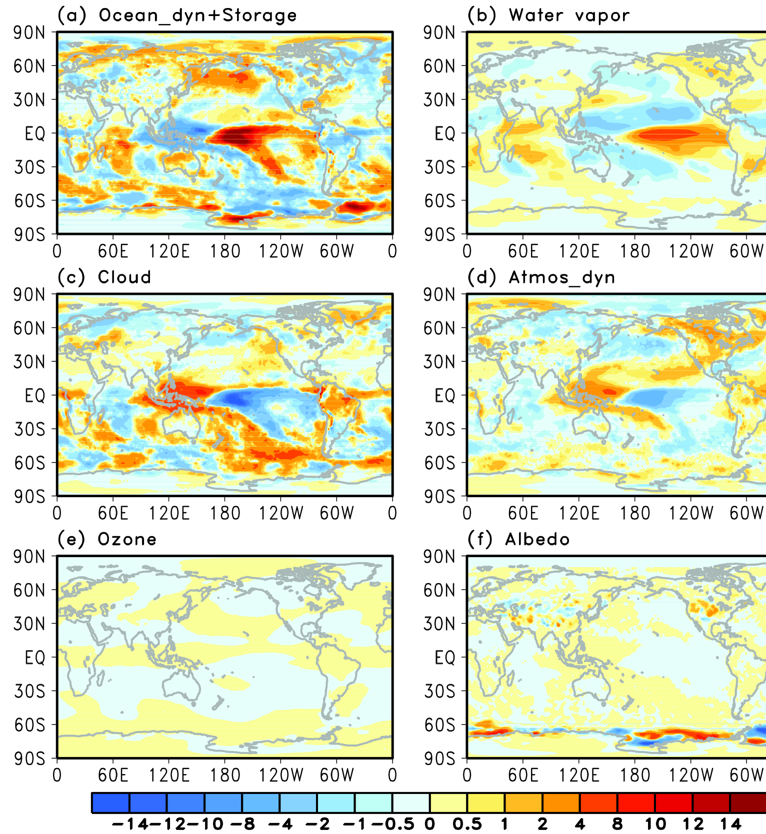

Fig. 2. Partial temperature anomalies in a composite El Niño state due to oceanic dynamics and heat storage anomalies (a), water vapor feedback (b), cloud feedback (c), atmospheric dynamical feedback (d), ozone feedback (e) and surface albedo feedback (f). Unit is *K*. (Adapted from Deng et al. 2012a)

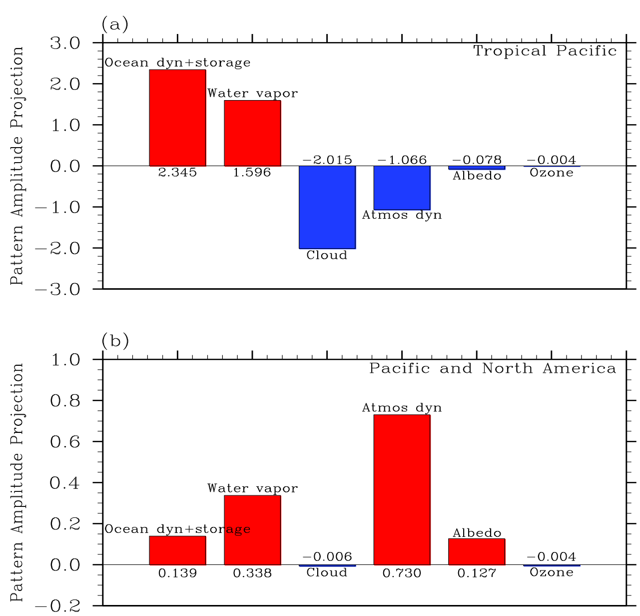

Fig. 3. Pattern-amplitude projections (PAPs) of the 6 partial temperature anomalies onto the observed El Niño SST pattern (a) and the PNA surface temperature pattern (b). Unit is *K*. (Adapted from Deng et al. 2012)

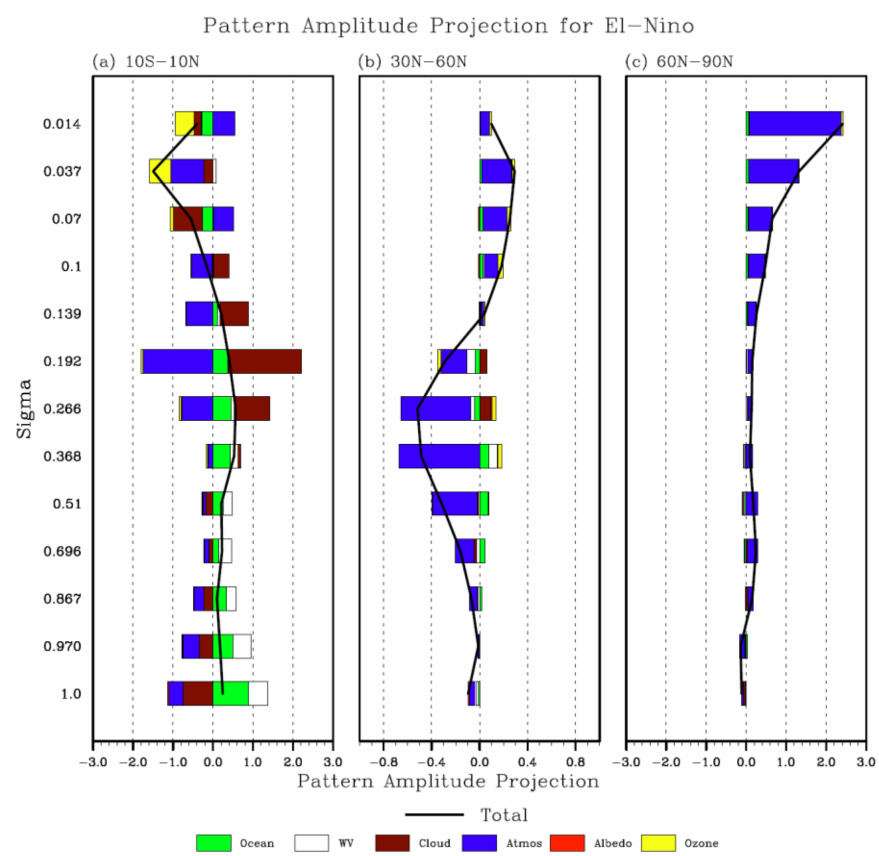

Fig. 4. Partitioning of the zonal-mean surface (sigma=1) and multi-level atmospheric temperature anomalies in a composite El Niño winter into contributions from various feedback processes based on the pattern-amplitude projections (PAPs) for the tropics (a), midlatitudes (b) and polar region (c). Unit is *K*. (Adapted from Park et al. 2012)

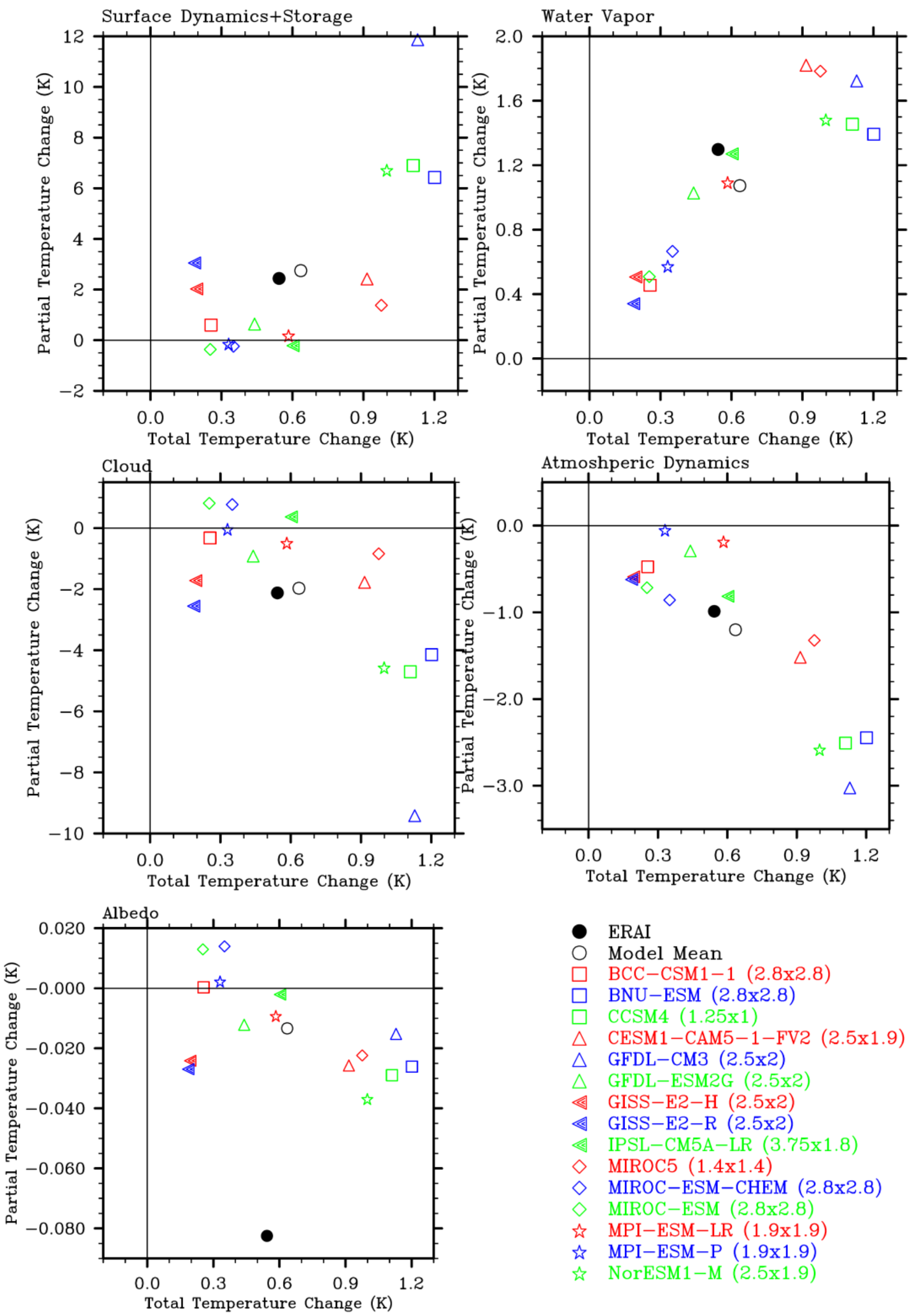

Fig. 5. Partial surface temperature change associated with surface dynamics, water vapor, cloud, atmospheric dynamics, and albedo changes as a function of total surface temperature change over the equatorial Pacific during El Niño in ERA-Interim and in multiple CMIP5 models' historical climate simulations. (Adapted from Park et al. 2014b)

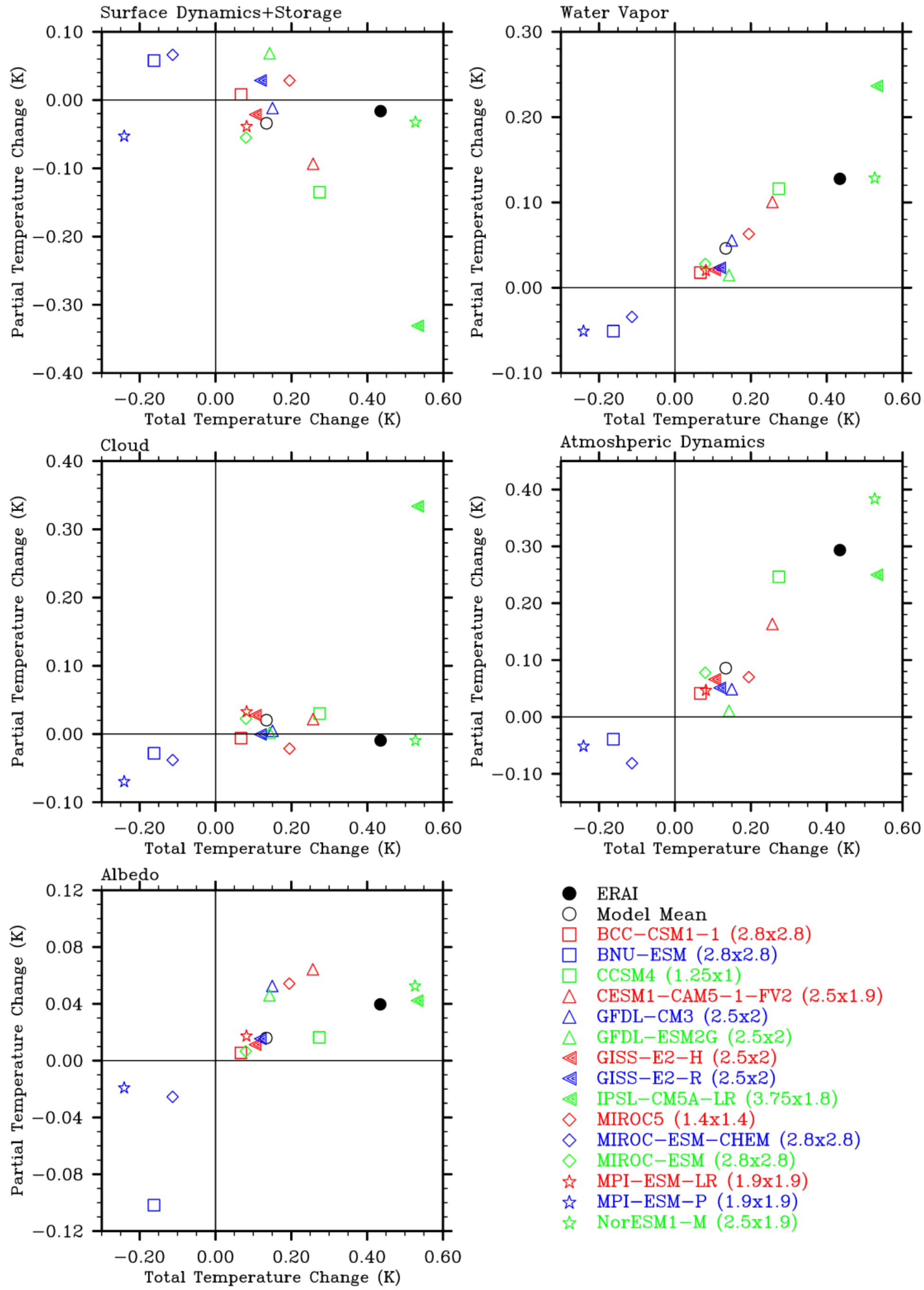

Fig. 6. Partial surface temperature change associated with surface dynamics, water vapor, cloud, atmospheric dynamics, and albedo changes as a function of total surface temperature change over the PNA region (see definition in Figure 1) during El Niño in ERA-Interim and in multiple CMIP5 models' historical climate simulations. (Adapted from Park et al. 2014b)

2. Process-level attribution of 3D atmospheric and surface temperature anomalies related to NAM variability

As reported in Deng et al. (2013), the local temperature anomaly associated with the Northern Annular Mode (NAM) variability in boreal winter in the ERA-Interim reanalysis is decomposed into partial temperature anomalies due to changes in atmospheric dynamics, water vapor, clouds, ozone, surface albedo, and surface dynamics with the CFRAM method. As shown in Figure 7, large-scale ascent/descent as part of the NAM-related mean meridional circulation anomaly adiabatically drives the main portion of the observed zonally averaged atmospheric temperature response, particularly the tropospheric cooling/warming over northern extratropics. Contributions from diabatic processes are generally small but could be locally important, especially at lower latitudes where radiatively active substances such as clouds and water vapor are more abundant. For example, in the tropical upper troposphere and stratosphere, both cloud and ozone forcings are critical in leading to the observed NAM-related temperature anomalies. For surface temperature anomalies over different regions (Figure 8), radiative forcing due to changes in water vapor acts as the main driver of the surface warming of southern North America during a positive phase of NAM, with atmospheric dynamics providing additional warming. In the negative phase of NAM, surface albedo change drives the surface cooling of southern North America, with atmospheric dynamics providing additional cooling. Over the subpolar North Atlantic and northern Eurasia, atmospheric dynamical processes again become the largest contributor to the NAM-related surface temperature anomalies, although changes in water vapor and clouds also contribute positively to the observed surface temperature anomalies while change in surface dynamics contributes negatively to the observed temperature anomalies.

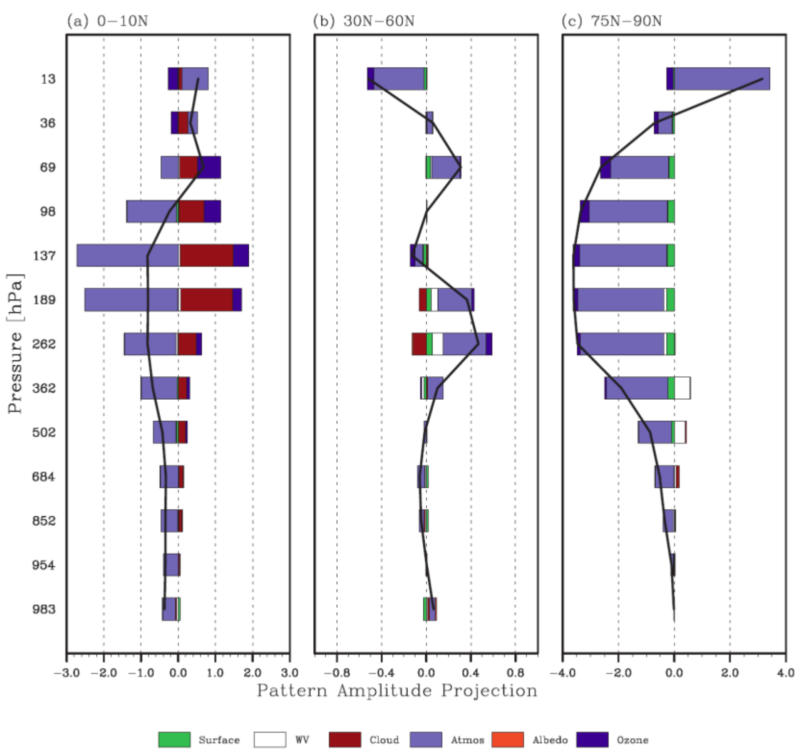

Fig. 7. Vertical profile of the PAP coefficients (color bars) associated with various radiative and dynamical forcing of the NAM+ (positive NAM phase) temperature anomalies (K) in (a) 0°–10°N, (b) 30°–60°N, and (c) 75°–90°N. The solid black curves indicate the vertical profiles of the observed temperature anomalies averaged over the respective zonal belts. (Adapted from Deng et al. 2013)

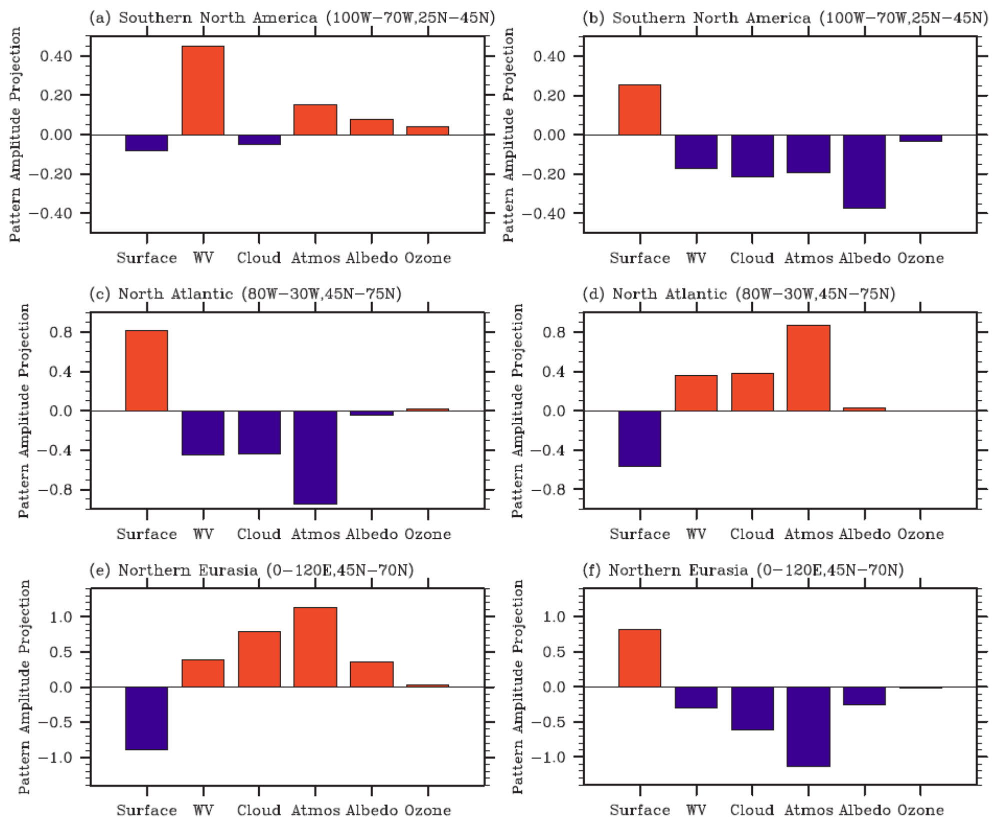

Fig. 8. PAP coefficients associated with various radiative and dynamical forcing of the area-averaged surface temperature anomalies (K) over (a),(b) southern North America, (c),(d) North Atlantic, and (e),(f) northern Eurasia. The left (right) column corresponds to the composite NAM+ (NAM-) month. (Adapted from Deng et al. 2013)

3. Feedback attribution of the mean temperature biases in CMIP5 models

Most recently, we have adopted the CFRAM to dissect and obtain process-level understanding of the annual mean surface temperature biases in the NCAR Community Earth System Model version 1 (CESM1) (Park et al. 2014a). Figure 9 below shows the decomposition of the surface temperature biases of CESM1 into components related to model errors in representing surface albedo, water vapor, clouds, sensible/latent heat flux, dynamics of land surface/ocean processes, and dynamics of atmospheric processes. The spatial distributions of temperature biases of radiative and non-radiative (dynamical) origins are given in Figure 10, where the relative importance of errors of each origin (i.e., radiative-error-dominant or dynamical-error-dominant) are also highlighted for each location around the world. This decomposition results provide direct guidance for model dynamics/physics tuning targeting better simulation of regional surface and atmospheric temperatures and we are currently extending the analysis to consider various seasons and also more CMIP5 participating models.

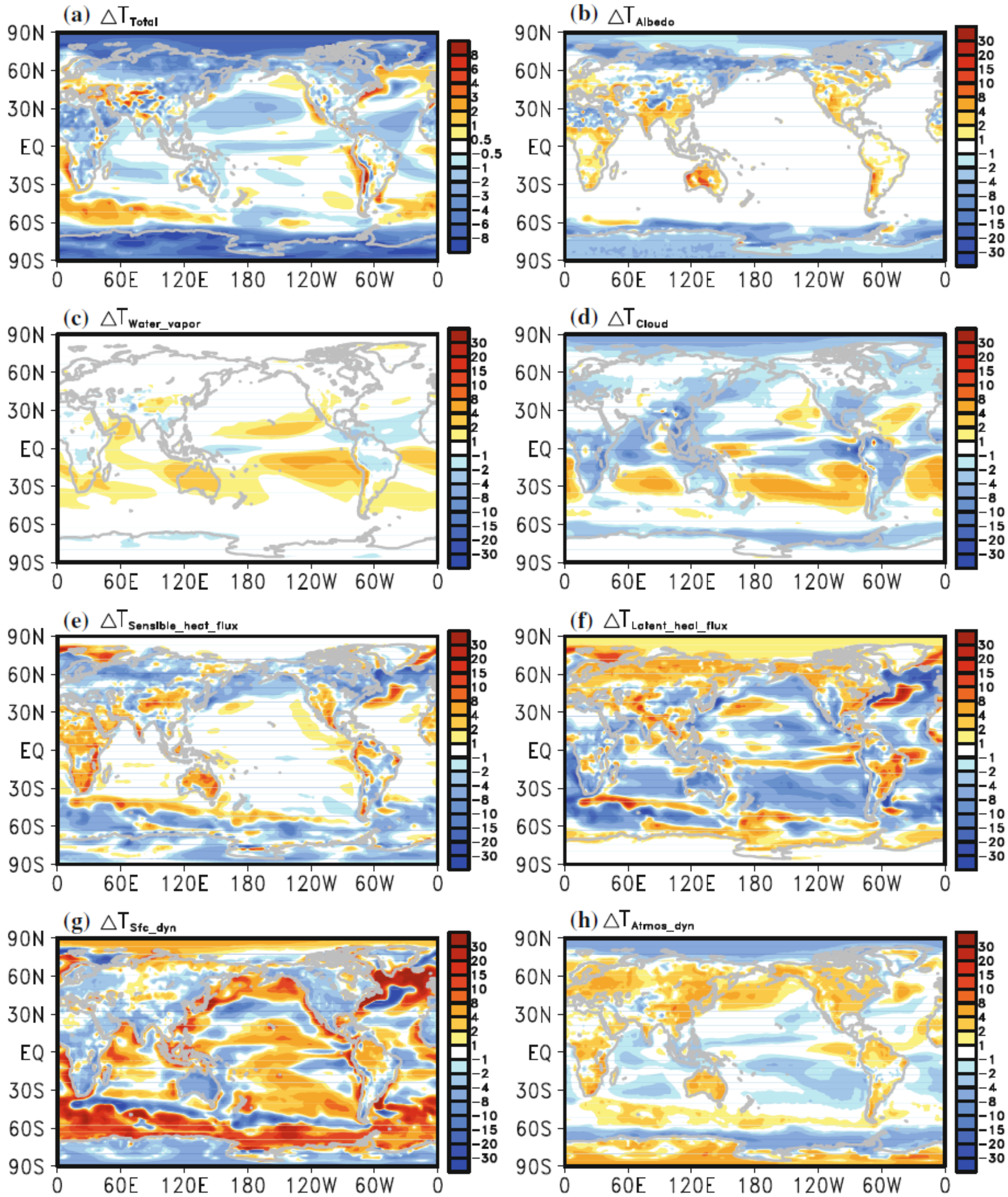

Fig. 9. (a) The annual-mean CESM1 model surface temperature biases (unit: K). The decomposition of the total temperature bias into components related to model bias in (b) albedo, (c) water vapor, (d) cloud, (e) sensible heat flux, (f) latent heat flux, (g) surface dynamics (land and ocean), and (h) atmospheric dynamics. (Adapted from Park et al. 2014a).

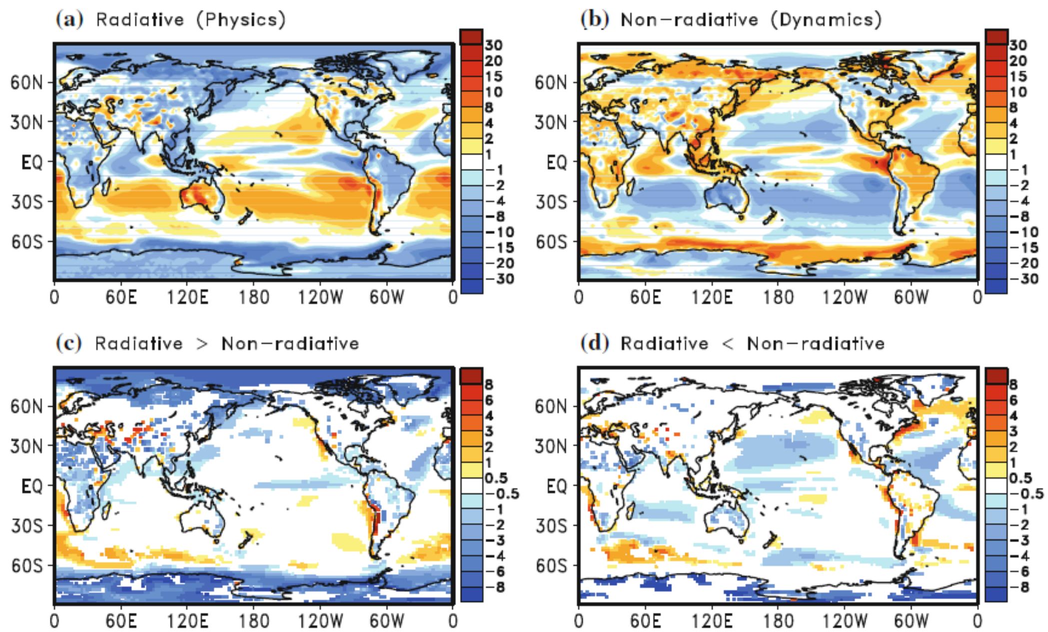

Fig. 10. The annual-mean CESM1 model surface temperature biases due to (a) radiative (sum of water vapor, cloud, and albedo) processes (physics), and (b) non-radiative (sum of sensible/latent heat flux, surface dynamics, and atmospheric dynamics) processes (dynamics). The sum of partial temperature biases where radiative processes are more dominant than non-radiative processes (c), and where non-radiative processes are more dominant (d). Unit: K. (Adapted from Park et al. 2014a)

4. Additional research at Georgia Tech supported by the DOE grant

In addition to the ENSO and NAM analysis, this DOE grant at Georgia Tech also supported a study that explores the use of graphical models for causal discovery in the inter-connections among various modes of low-frequency variability in the northern extratropics and the construction of a causal discovery-based climate network that emphasizes information flow in the climate system (Ebert-Uphoff and Deng 2012a; 2012b; Deng and Ebert-Uphoff 2014). Specifically, constraint based structure learning is applied to derive hypotheses of causal relationships between four prominent modes of atmospheric low-frequency variability in boreal winter including the Western Pacific Oscillation (WPO), Eastern Pacific Oscillation (EPO), Pacific North America Pattern (PNA) and North Atlantic Oscillation (NAO). The results are shown in the form of static and temporal independence graphs, also known as Bayesian Networks. It is found that WPO and EPO are nearly indistinguishable from the cause-effect perspective as strong simultaneous coupling is identified between the two. In addition, changes in the state of EPO (NAO) may cause changes in the state of NAO (PNA) approximately 18 (3-6) days later (Figure 11). These results are not only consistent with previous findings on dynamical processes connecting different low-frequency modes (e.g., interaction between synoptic and low-frequency eddies), but also provide basis for formulating new hypotheses regarding the time-scale and temporal-sequencing of dynamical processes responsible for these connections. When applying this method to global, daily 500mb geopotential height data in the NCEP/NCAR reanalysis, we were able to build a new type of climate network that reveals major "information pathways" in the climate system. Further analysis for the NCAR CCSM4 future climate projection under RCP8.5 scenario indicates that as the climate warms, major midlatitude information pathways will drift poleward and tropical information pathways start diminishing (Figure 12). These results provide a unique angle to understand complicated coupled dynamics in the Earth's climate system and we are currently extending such analysis to understand vertical propagation of large-scale waves in the tropical atmosphere.

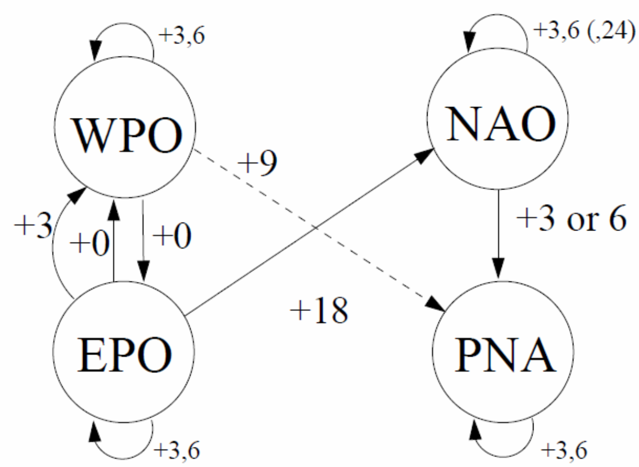

Fig. 11. Summary diagrams showing the causal relations among WPO, EPO, NAO, and PNA. The arrows indicate the direction of information flow, thus the cause-effect relationship, and the numbers indicate the time lead/lag in days. (Adapted from Ebert-Uphoff and Deng 2012a)

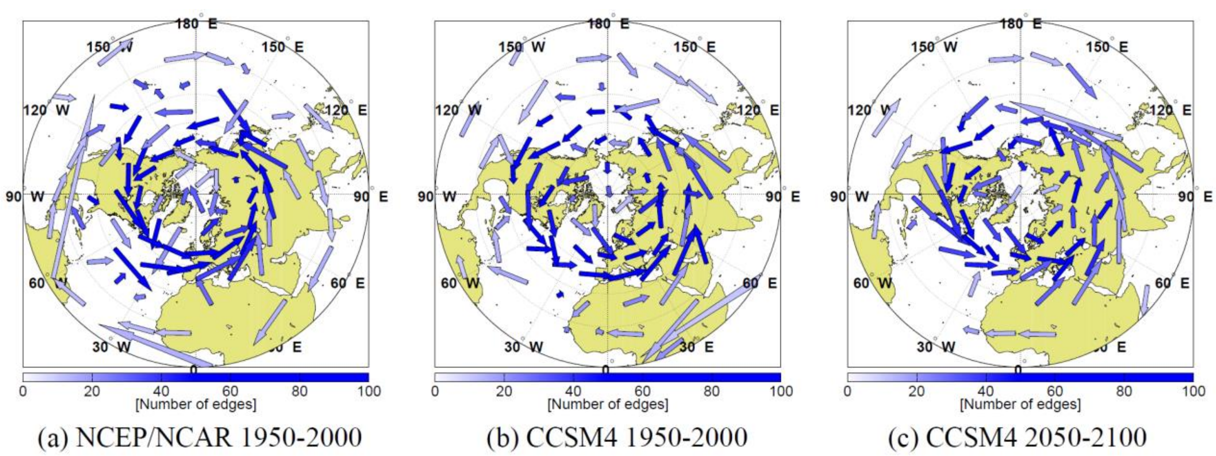

Fig. 12. The average velocity of information flow (in km/day) for boreal winter derived from the NCEP/NCAR reanalysis for the period 1950-2000 (a), CCSM4.0's 20th century climate simulation for the period 1950-2000 (b), and CCSM4.0's 21st century climate projection for the period 2050-2100 (c). The length of an arrow corresponds to the distance across which the information travels in a 24-hour period and color shading of the arrow indicates the overall level of activity of the information pathway. (Adapted from Deng and Ebert-Uphoff 2014)

In addition to the above work that introduced causal discovery with probabilistic graphical models to the climate community, this DOE grant also partly supported research at Georgia Tech that 1) examined the interaction between East Asian anthropogenic aerosols and atmospheric transients over the North Pacific in boreal winter (Zhou et al. 2013); 2) evaluated the climatology and interannual variability of the local kinetic energy budget of the Northern Hemisphere high-frequency and intermediate-frequency atmospheric eddies (Jiang et al. 2013); 3) conducted synoptic and dynamical characterization of East Asian cold surge events (Park et al. 2013); 4) examined the stratospheric pathway of tropical-polar interaction in the NCAR WACCM model (Hegyi et al. 2014); and 5) investigated the remote forcing of western U.S. atmospheric river activities by East Asian cold surges and highlighted the critical role of intermediate-frequency (10-30day) atmospheric disturbances in establishing such connections in both observations and in high resolution simulations made with the NCAR CCSM4 model (Jiang et al. 2014).

7. Project Participants:

Dr. Tae-Won Park, Postdoctoral Fellow at Georgia Tech (02/2011 – present)
Tianyu Jiang, PhD candidate, graduate student at Georgia Tech (12/2012 – 06/2013)
Bradley Hegyi, PhD candidate, graduate student at Georgia Tech (01/2012 – present)

8. Publications:

1) **Deng, Yi**, Tae-Won Park, Ming Cai, 2012: Process-Based Decomposition of the Global Surface Temperature Response to El Niño in Boreal Winter. *J. Atmos. Sci.*, **69**, 1706–1712.
2) Park, T.-W., **Y. Deng**, and M. Cai, 2012: Feedback attribution of the El Niño–Southern Oscillation–related atmospheric and surface temperature anomalies, *J. Geophys. Res.*, 117, D23101, doi:10.1029/2012JD018468.
3) **Deng, Yi**, Tae-Won Park, Ming Cai, 2013: Radiative and Dynamical Forcing of the Surface and Atmospheric Temperature Anomalies Associated with the Northern Annular Mode. *J. Climate*, **26**, 5124–5138.
4) Ebert-Uphoff, I. and **Y. Deng**, 2012b: A new type of climate network based on probabilistic graphical models: Results of boreal winter versus summer, *Geophys. Res. Lett.*, **39**, L19701, doi:10.1029/2012GL053269.
5) Ebert-Uphoff, I. and **Y. Deng**, 2012a: Causal discovery for climate research using graphical models. *J. Climate*, **25**, 5648-5665.
6) Park, T., C. Ho and **Y. Deng**, 2013: A synoptic and dynamical characterization of wave-train and blocking cold surge over East Asia. *Clim. Dyn*. doi: 10.1007/s00382-013-1817-6.
7) Park, T.-W., Y**. Deng**, M. Cai, J. Jeong, and R. Zhou, 2013: A dissection of the surface temperature biases in the Community Earth System Model Version 1.0. *Clim. Dyn.* doi: 10.1007/s00382-013-1920-8.
8) Jiang, T., **Y. Deng**, and W. Li, 2013: Local kinetic energy budget of high-frequency and intermediate-frequency eddies: winter climatology and interannual variability. *Clim. Dyn.*, **41**, 961-976, doi: 10.1007/s00382-013-1684-1.
9) Zhou, R., and **Y. Deng**, 2013: A model analysis of the interactions between East Asian anthropogenic aerosols and North Pacific atmospheric transients in boreal winter. *J. Geophys. Res.*, **118**, 306–316, doi:10.1029/2012JD018649.
10) **Deng, Y.**, and I. Ebert-Uphoff, 2014: Weakening of atmospheric information flow in a warming climate in the Community Climate System Model, *Geophys. Res. Lett.*, **41**, doi:10.1002/2013GL058646.
11) Hegyi, B., **Y. Deng**, R. Black, and R. Zhou, 2014: Initial and transient response of the winter polar stratospheric vortex to idealized equatorial Pacific sea surface temperature forcing in the NCAR WACCM model. *J. Climate*, **27**, 2699-2713.
12) Jiang, T., K. J. Evans, **Y. Deng**, and X. Dong, 2014: Intermediate frequency atmospheric disturbances: A dynamical bridge connecting western U.S. extreme precipitation with East Asian cold surges. *J. Geophys. Res.*, **119**, 3723-3735, doi: 10.1002/2013JD021209.
13) Sejas, S. A., O. S. Albert, M. Cai, and **Y. Deng**, 2014: Feedback attribution of the land-sea warming contrast in a global warming simulation of the NCAR CCSM4. *Environ. Res. Lett*. (In press)
14) Park, T., J. Jeong, **Y. Deng**, R. Zhou, and M. Cai, 2014a: Quantitative decomposition of radiative and non-radiative contributions to temperature anomalies related to Siberian High variability. *Clim. Dyn.*, doi: 10.1007/s00382-014-2371-6.
15) Park, T., **Y. Deng**, and M. Cai, 2014b: Feedback attribution of ENSO surface temperature anomalies in CMIP5 modes. *J. Climate* (To be submitted)

9. Presentations/Meetings Attended:

1) Deng, Y., T. Park, R. Zhou, and M. Cai: A dissection of the surface temperature biases in the Community Earth System Model, DOE Climate and Earth System Modeling PI meeting, Washington, DC, May 2014.
2) Park, T., Y. Deng, and M. Cai: Radiative and dynamical forcing of El-Niño-related global temperature anomalies in the observations and in CMIP5 models, DOE Climate and Earth System Modeling PI meeting, Washington, DC, May 2014.
3) Hegyi, B., and Y. Deng: Contributions of atmospheric transients to the recent changes in summer Arctic sea ice extent, AMS annual meeting, Atlanta, February 2014.
4) Jiang, T., Y. Deng, and K. J. Evans: The role of atmospheric rivers in linking weather extremes: East Asian cold surge and high impact precipitation over the west coast of U.S., AMS annual meeting, Austin, January 2013.
5) Hegyi, B., Y. Deng, R. Black, anda R. Zhou: Initial Transient Response of the Polar Stratospheric Vortex to Idealized Equatorial Pacific Sea Surface Temperature Anomalies in WACCM, AMS annual meeting, Austin, January 2013.
6) Deng, Y., T. Park, and M. Cai: Radiative and Dynamical Forcing of the Surface and Atmospheric Temperature Anomalies Associated with the Northern Annular Mode, AMS annual meeting, Austin, January 2013.
7) Deng, Y., T. Park and M. Cai: Feedback decomposition of the global surface temperature response to El Nino in boreal winter, AMS annual meeting, New Orleans, LA, January 2012.
8) Park, T., Y. Deng and M. Cai: Process-Resolving Decomposition of the Global Temperature Response to the El Niño-Southern Oscillation, AGU fall meeting, San Francisco, CA, December 2011.
9) Deng, Y., T. Park and M. Cai: Feedback decomposition of the global surface temperature response to El Niño, DOE Climate and Earth System Modeling PI meeting, Washington, DC, September 2011.